

Deposition and Characterization of $\text{Cu}_2\text{ZnSnS}_4$ Thin Films for Solar Cell Applications

Nabeel A. Bakr*, Sabah A. Salman, Sabreen A. Hameed

Department of Physics, College of Science, University of Diyala, Diyala, Iraq.

Abstract

Copper zinc tin sulfide (CZTS) thin films have been grown on glass substrates at 400 °C by using chemical spray pyrolysis as relatively fast and vacuum-free method. The Spray solutions were prepared with different molar concentrations of copper chloride dihydrate, zinc chloride, tin chloride dihydrate while the concentration of thiourea was kept constant. The thickness of the prepared thin films was about (400 nm) measured by gravimetric method. The structural, optical and electrical properties of the prepared films have been studied using XRD, Raman spectroscopy, UV-Vis-NIR spectroscopy and Hall measurement. The crystallite size of CZTS films was estimated using Scherrer's formula and it was found that the CZTS thin films have maximum crystallite size of (16.03 nm) at concentration ratio ($\text{Cu}/(\text{Zn}+\text{Sn})=1.4$) which is related to the film (CZTS_5). Williamson–Hall analysis was carried out for all samples and the crystallite size and microstrain were estimated. Raman shift measurement showed that the main peaks of the films are located at ($330\text{-}335\text{ cm}^{-1}$). The absorbance and transmittance spectra were recorded in the wavelength range of (350- 900) nm in order to study the optical properties. The optical energy gap for allowed direct electronic transition was (1.5-2.1) eV with a high absorption coefficient ($\alpha >10^4\text{ cm}^{-1}$) and it is suitable for solar cell applications. The conductivity of CZTS films was estimated using Hall measurement and it is found that the CZTS thin films have maximum conductivity of $2.3573(\Omega.\text{cm})^{-1}$ at concentration ratio ($\text{Cu}/(\text{Zn}+\text{Sn})=1$).

Keywords: CZTS thin films, Optical properties, XRD, Raman spectroscopy, Hall measurements.

INTRODUCTION

For the last several decades, world energy consumption has substantially increased, and it is expected to continue increasing in the near future [1]. Solar cells based on semiconductor thin films are promising as alternative to silicon. The quaternary compound $\text{Cu}_2\text{ZnSnS}_4$ (CZTS) is a promising material for low-cost absorber layers in thin film solar cells applications due to its suitable optoelectronic properties (p-carrier type, direct band gap of 1.4-1.5 eV and high optical absorption coefficient $>10^4\text{ cm}^{-1}$), elemental availability, and nontoxicity of its constituents [2-5]. It is basically derived from CuInS_2 (CIS) by substitution of two in atoms with one Zn and one Sn atom. This isoelectronic substitution produces a material with many of the same properties of the parent compound, but one that crucially no

longer contains any rare or expensive elements. $\text{Cu}_2\text{ZnSnS}_4$ compounds may exist in two main crystal structures, known as kesterite and stannite [6-9], both are tetragonal structures, arranged in a cubic closed packed array of sulphur anions, with cations occupying one half of the tetrahedral voids, with a stacking similar to zinc blende. The structural differences are related to a different order in the cation sublattice. Kesterite is characterized by alternating cation layers of CuSn, CuZn, CuSn and CuZn at $z=0, 1/4, 1/2$ and $3/4$, respectively, whereas in stannite structure, ZnS layers alternate with Cu_2 layers. Tin and sulphur ions occupy the same lattice positions in both structures. The different deposition methods applied in the fabrication of CZTS thin films (atom beam sputtering, thermal evaporation, hybrid sputtering, pulsed laser deposition, photochemical deposition, screen printing, electron beam evaporation) require complicated equipment and are expensive. In the present work, the aim is to use the spray pyrolysis as one of the methods which are non-toxic, cheap, fast and vacuum-free [10-12].

EXPERIMENTAL

$\text{Cu}_2\text{ZnSnS}_4$ (CZTS) thin films were deposited on soda-lime glass substrates by chemical spray pyrolysis. The glass substrates were cleaned ultrasonically in distilled water, acetone, and distilled water respectively for (10 min) of each step and then dried by wiping them with soft paper. Spray solution was prepared by mixing aqueous solutions of copper chloride dihydrate ($\text{CuCl}_2.2\text{H}_2\text{O}$), zinc chloride (ZnCl_2), tin chloride dihydrate ($\text{SnCl}_2.2\text{H}_2\text{O}$) and thiourea ($\text{SC}(\text{NH}_2)_2$) with a final volume of 100 mL. Table (1) shows the molar concentrations of the solutions prepared at different ratios of $\text{Cu}/(\text{Zn}+\text{Sn})= (0.6, 0.8, 1, 1.2 \text{ and } 1.4)$. Excess thiourea was used to compensate the loss of sulphur during pyrolysis. Mixing the solutions is carried out by using (Magnetic Stirrer) and leaving the solution for one hour to make sure that no residues are left and to ensure the homogeneity of the resultant solution. The solution was sprayed to the substrate which was kept at constant temperature of 400°C using filtered air as carrier gas at a flow rate of 5 mL/min. To prevent the substrate from excessively cooling, the prepared solution was sprayed on the substrate for 10 s with 2 min intervals. Other deposition conditions such as spray nozzle substrate distance (30 cm) and pressure of the carrier gas (1.5 bar) are kept constant for all samples. When the solution is sprayed, the reaction takes place at the surface of the heated substrate. The resultant films are stable and have good adhesive properties with a uniform thickness of (400) nm

Table 1: Molar concentrations of solutions used to prepare CZTS films.

Sample Code	Cu/(Zn+Sn)	CuCl ₂ .2H ₂ O (M)	ZnCl ₂ (M)	SnCl ₂ .2H ₂ O (M)	SC(NH ₂) ₂ (M)	
<i>Cu-poor</i>	CZTS ₁	0.6	0.032	0.024	0.024	0.16
	CZTS ₂	0.8	0.036	0.022	0.022	0.16
	CZTS ₃	1	0.040	0.020	0.020	0.16
	CZTS ₄	1.2	0.044	0.018	0.018	0.16
<i>Cu-rich</i>	CZTS ₅	1.4	0.048	0.016	0.016	0.16

measured by gravimetric method using sensitive electronic balance (Mettler, AE - 160) with four digits sensitivity (10⁻⁴ g). The substrates are weighted before and after deposition. From the weight difference and the area of substrate, the thin film thickness (t) can be measured, according to the following equation

$$t = \frac{\Delta m}{\rho A} \dots (1)$$

Where Δm is the weight difference of substrate (g), A is the area of the thin film (cm²), ρ is the density of material of the thin film. The structural properties were determined by X-ray diffraction (XRD; Shimadzu 6000) with CuK α radiation ($\lambda = 1.5406 \text{ \AA}$) as the source. Raman Spectra were obtained at backscattering configuration using (Jobin-Yvon Horiba Labram800). The optical transmission and absorption spectra of the CZTS thin films were measured by (Shimadzu,

UV- 1800) in the wavelength range of (350 – 900) nm. Hall effect measurement was obtained by using (HMS 3000).

RESULTS AND DISCUSSION

The XRD patterns for CZTS thin films are recorded and they are illustrated in Figure (1). From the figure, it can be noticed that all the patterns exhibit diffraction peaks around (2 θ ~23°, 28°, 32°, 47° and 56°) referred to (110), (112), (200), (220) and (312) favorite directions respectively which is in agreement with the International Center of Diffraction Data (ICDD) card number 26-0575. The strongest peak occurs at 2 θ ~28° which is referred to (112) plane. The presence of more than one diffraction peak and the positions of the peaks lead to the conclusion that the films are polycrystalline in nature with a tetragonal crystalline structure, which is in agreement with other reports [13,14].

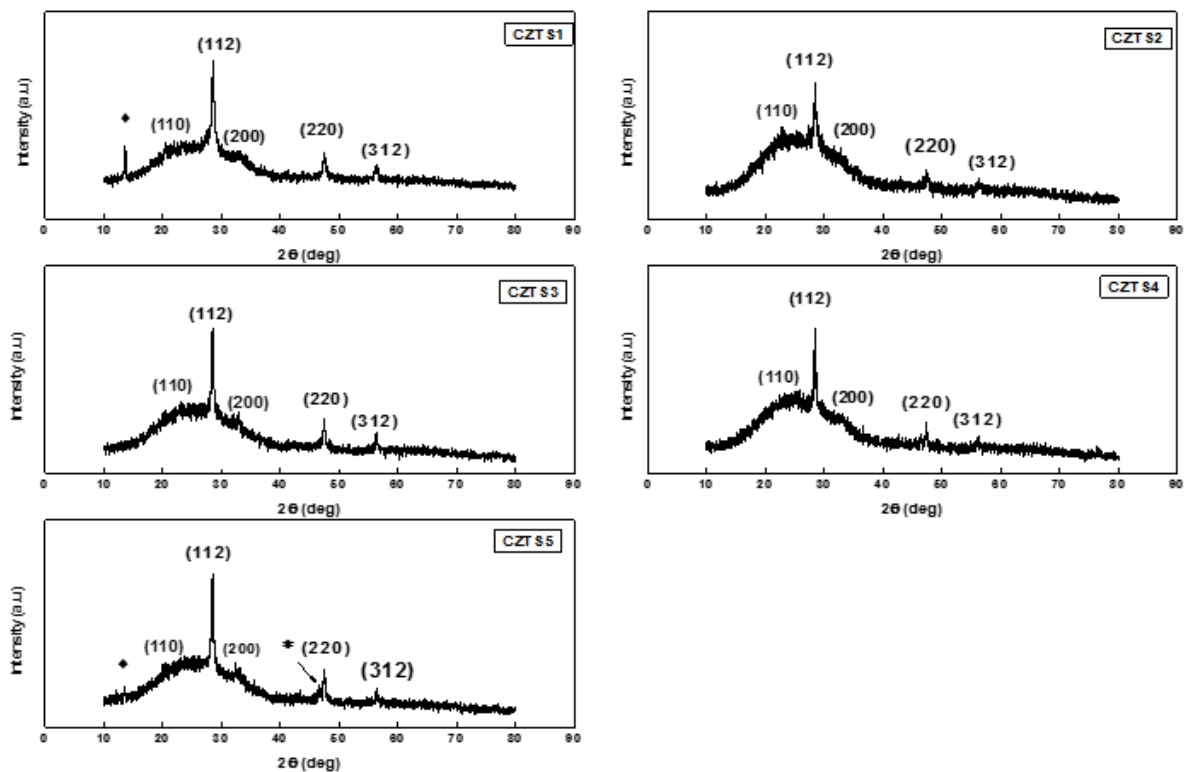


Figure 1: XRD patterns of the CZTS thin films at different Cu/(Zn+Sn) ratios.

Table 2: X-ray diffraction results of the CZTS thin films.

Sample		CZTS ₁	CZTS ₂	CZTS ₃	CZTS ₄	CZTS ₅
2θ (deg)		28.53	28.50	28.47	28.45	28.49
(FWHM)		0.0112	0.0149	0.0090	0.0089	0.0089
(rad)						
Lattice Parameters	(a=b)	0.5420	0.5420	0.5431	0.5431	0.5418
(nm)	(c)	1.084	1.084	1.094	1.086	1.087
(c/a)		2.000	2.000	2.014	1.999	2.006

In Tetragonal ideal structure, the ratio of the lattice vector (c/a) is 2, table (2) shows the ratios of the lattice vector (c/a) of the prepared films, the ratio less than 2 means that the lattice is compressed in the c-axis direction while the ratio greater than 2 means that the lattice is elongated along the c-axis, and the table also shows that the full width at half maximum (FWHM) values are different, indicating that crystallite size of CZTS films is affected by changing the ratio Cu/(Zn+Sn).

Larger grains are required to fabricate high efficiency solar cells. The increase of grain size decreases the grain boundaries that diminish recombination and thereby the effective diffusion length of the minority carriers is increased causing a higher short circuit photocurrent in polycrystalline solar cells [15]. The crystallite size (D) of these films is determined using Scherrer's formula [16]:

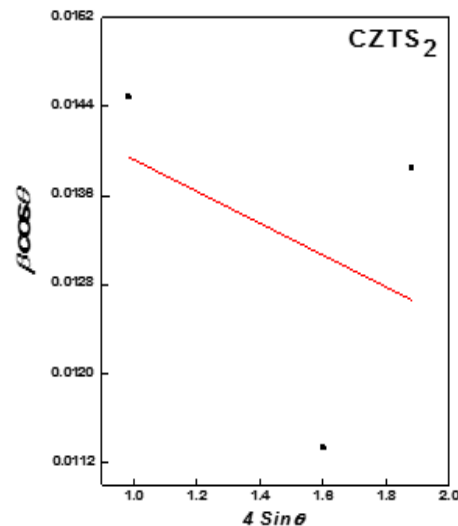
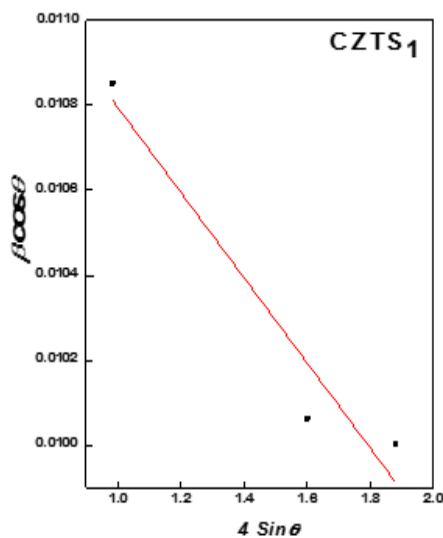
$$D = K\lambda / \beta \cos\theta \quad \dots (2)$$

Where K is the Scherrer's constant and is assumed to be equal

to 0.9, β is the full-width at half maximum (FWHM) and θ is the Bragg angle. In addition to the instrumental X-ray peak broadening, lattice strain and crystallite size are the other two independent factors that contribute to the total peak broadening. The strain induced broadening β_s is given by the relation β_s = 4εtanθ_{hkl}. Now the total peak broadening is represented by the sum of the contributions of crystallite size and strain present in the material. Assuming a uniform strain the W-H equation for the total peak broadening is given by:

$$\beta \cos\theta_{hkl} = k\lambda/D + 4\epsilon \sin\theta_{hkl} \quad \dots (3)$$

Where ε is the microstrain. A plot of 4sinθhkl along X-axis and βcosθhkl along Y-axis allows the estimation of the strain present in the material and the crystallite size from the slope and the intercept of the linear fit as shown in figure (2).



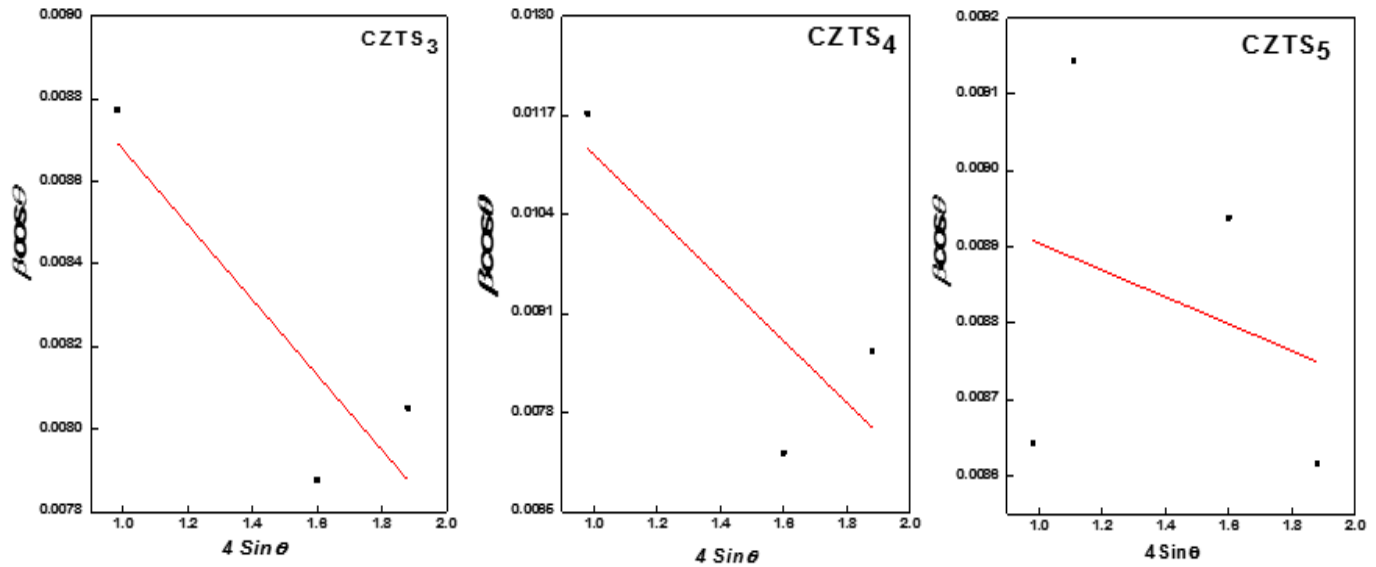


Figure 2: The W-H analysis for CZTS thin films.

The results of estimated average crystallite size of CZTS films depicted in table (3) show that the average crystallite size measured by Williamson–Hall are lower than those estimated by Scherrer’s method. The micro strains are induced during the growth of thin films, and will be raised from stretching or compression in the lattice. The strain broadening is caused by the displacements of the atoms with respect to their reference lattice positions [17]. The values of microstrain are negative for all samples which indicate the occurrence of compression in the lattice [18].

Table 3: Average crystallite size (measured by Scherrer’s method and Williamson–Hall analysis) and the microstrain of CZTS thin films.

Sample	D Scherrer (nm)	D W–H (nm)	Microstrain (S)
CZTS ₁	12.76	11.74	-0.0010
CZTS ₂	9.56	9.02	-0.0014
CZTS ₃	15.77	14.4	-0.0009
CZTS ₄	16.00	9.08	-0.0040
CZTS ₅	16.03	15.26	-0.0001

To investigate the phase purity of Cu₂ZnSnS₄, Raman shift measurements were carried out on films and the results are plotted in figure (3). The Raman spectra showed that the main peak of the samples is located at (330-335) cm⁻¹ which has been attributed to the kesterite CZTS. The presence of the peak near 282 cm⁻¹ proves the formation of CZTS single phase [19]. These peaks arise from A1 vibration mode, where only S-anions are involved [20,21]. Raman spectrum of CZTS₁ film showed peaks at 330 cm⁻¹ and 306 cm⁻¹ which are related to Cu₂ZnSnS₄ and Sn₂S₃ respectively. The samples CZTS₂, CZTS₃ and CZTS₄ showed peaks at (285,335) cm⁻¹, (282,331) cm⁻¹ and (285,332) cm⁻¹ respectively. These peaks are related to Cu₂ZnSnS₄ compound. CZTS₅ peaks at (306, 333 and 363) cm⁻¹ are assigned to Sn₂S₃, Cu₂ZnSnS₄ and Cu₂SnS₃ respectively, these results are quite consistent with the XRD patterns. There are several factors that could contribute to the change of the Raman peak position such as phonon confinement, strain, nonhomogeneity of the size distribution, defects and nonstoichiometry [22].

The optical properties of the prepared thin films have been investigated by using UV-Vis-NIR absorbance spectra in the region of (350-900) nm. Figure (4) shows the transmittance spectra as a function of the wavelength of Cu₂ZnSnS₄. The figure shows that the transmittance for all thin films increases rapidly as the wavelength increases in the range of (350-800) nm, and then increases slowly at higher wavelengths.

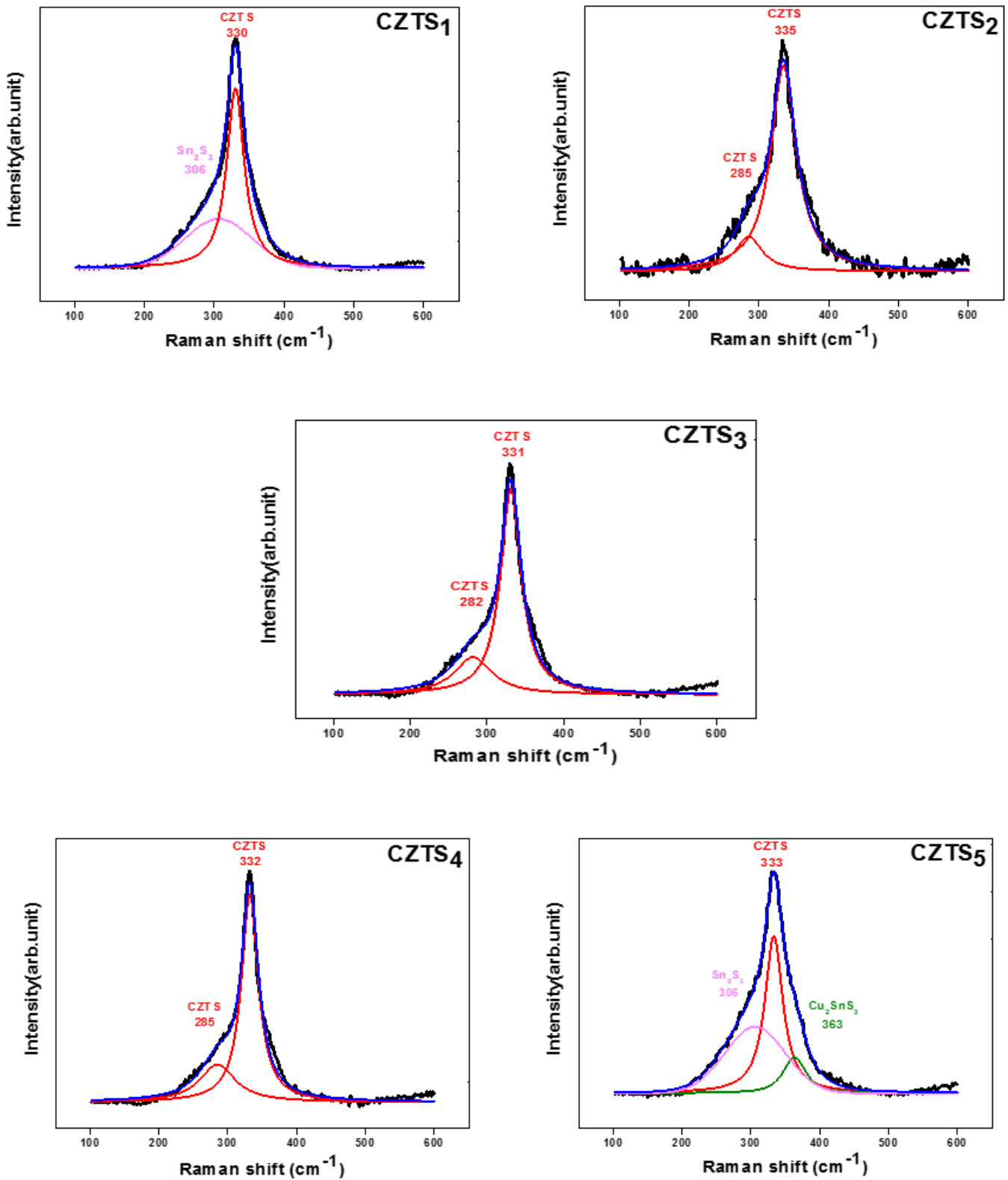


Figure 3: Raman shift at different Cu/(Zn+Sn) ratios.

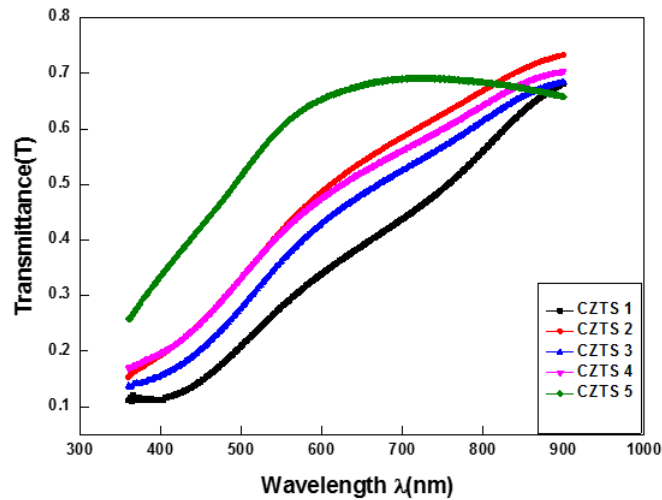


Figure 4: The transmittance of CZTS thin films as a function of wavelength.

Figure (5) shows the optical absorption coefficient as a function of incident photon energy of CZTS films. It has been noticed that all the prepared thin films have high absorption coefficient ($\alpha > 10^4 \text{ cm}^{-1}$) which indicates the increase of the probability of the occurrence of direct transitions. The Figure shows that the absorption coefficient of the film increases gradually with increase in photon energy. This evident

increase is due to the interaction of the material electrons with the incident photons which have enough energy for the occurrence of electron transitions. The difference in absorption coefficient values at every wavelength might be due to difference in $\text{Cu}/(\text{Zn}+\text{Sn})$ ratio, the reason for this is due to the difference in the amount of photons absorbed by the atoms.

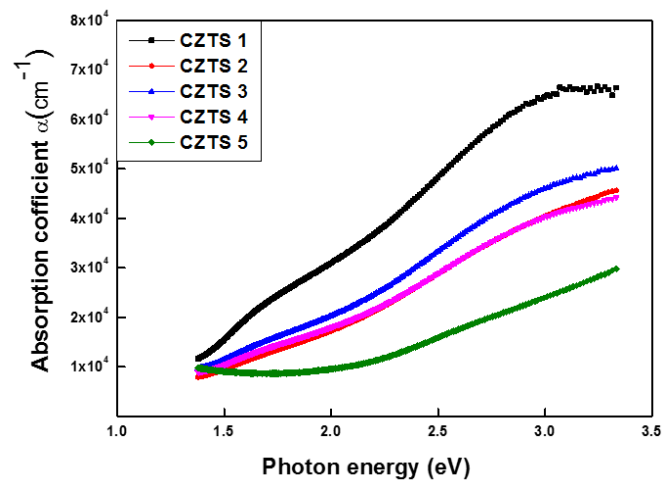


Figure 5: The absorption coefficient of CZTS thin films as a function of photon energy.

To evaluate the optical band gap for deposited films, the Tauc's formula was used [23]:

$$\alpha h\nu = A(h\nu - E_g)^{1/2} \quad \dots (4)$$

Where $h\nu$: is the photon energy, A : is a temperature independent constant that depends on the effective mass and the refractive index, E_g : is the energy gap. Using the linear extrapolation method, the E_g values are (1.5, 1.77, 1.56, 1.71 and 2.16) eV for the films CZTS₁, CZTS₂, CZTS₃, CZTS₄ and

CZTS₅ respectively. As seen in Figure (6) there is no obvious correlation between the value of band gap and copper content in films. This could be due to the various factors that simultaneously affect the CZTS band gap such as the non-stoichiometry, the nature and the amount of secondary phases and in some extent, the variations in morphology.

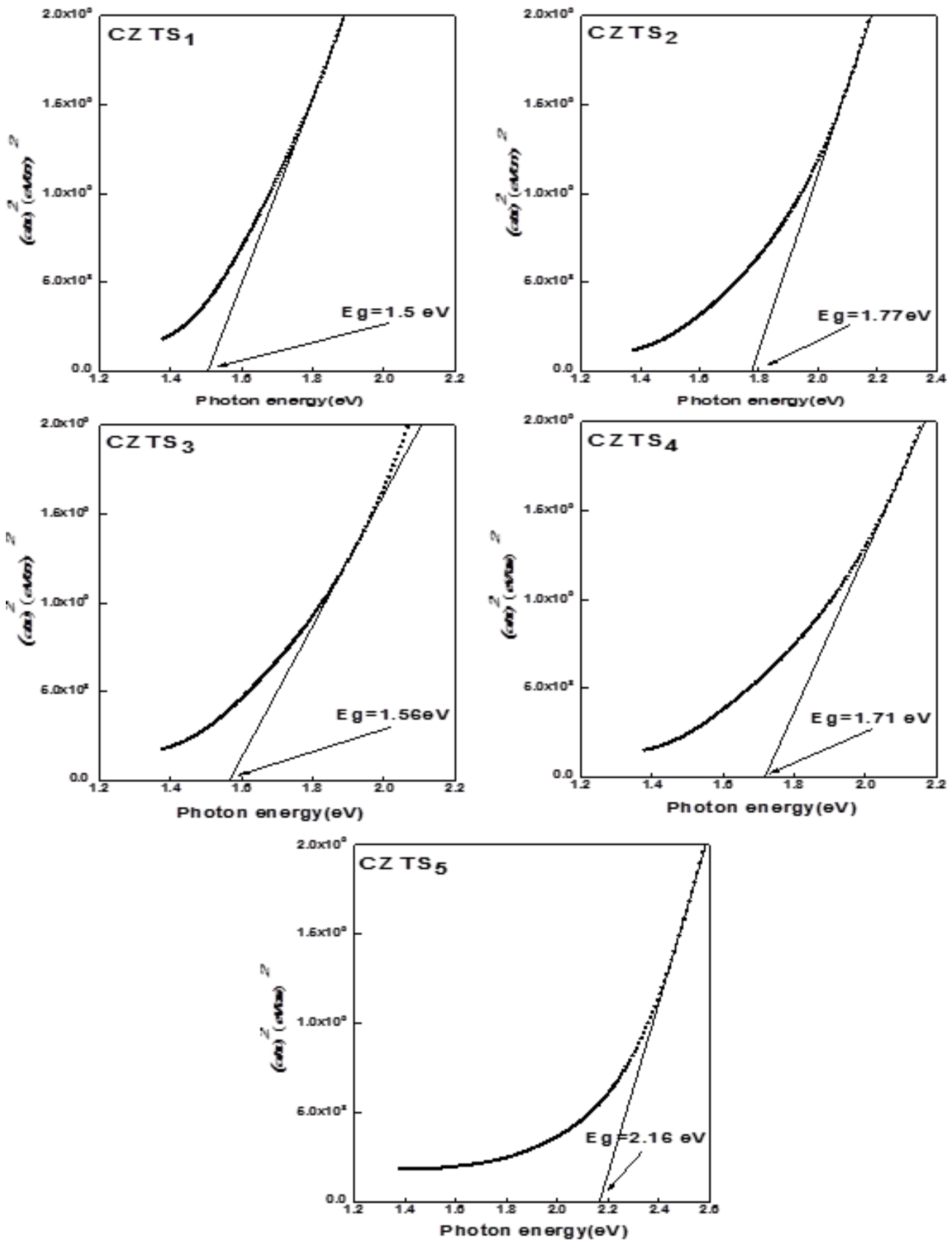


Figure 6: The relation between $(\alpha h\nu)^2$ and $h\nu$ of CZTS thin films.

Urbach energy (Eu) can be calculated by using the equation:

$$\alpha = \alpha_0 \exp\left(\frac{h\nu}{E_u}\right) \quad \dots (5)$$

Where α_0 : is a constant that depends on the type of transitions. The values of Urbach energy (Eu) are obtained from the inverse of the slope of linear part of $(\ln\alpha)$ vs $(h\nu)$ plot as

shown in Figure (7). Urbach energy values are 387, 595, 589, 624 and 1040.8 meV for samples CZTS₁, CZTS₂, CZTS₃, CZTS₄ and CZTS₅ respectively. Urbach energy is related to density of localized states induced by structural defects.

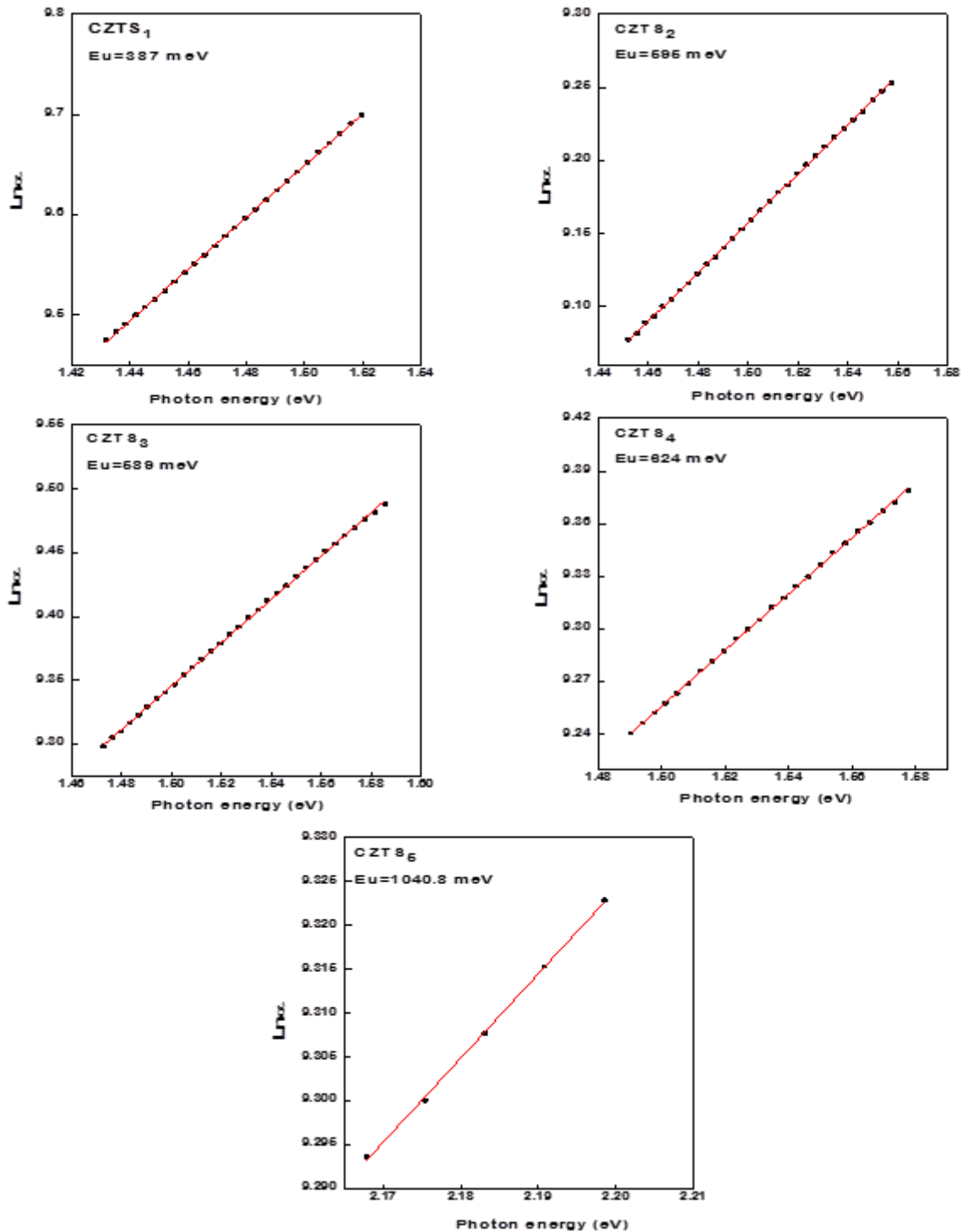


Figure 7: The Urbach plots of the (CZTS) thin films.

Hall effect measurement at 300K revealed p-type conductivity with a high concentration of free holes ($p_{\text{Hall}} 66.54 \times 10^{17} \text{cm}^{-3}$) and low mobility ($\mu_{\text{Hall}} \sim 2.21 \text{cm}^2/\text{V.s}$), the maximum value of conductivity is $2.3573 (\Omega \cdot \text{cm})^{-1}$ which belongs to the film CZTS₃ as shown in table(4). Recent studies showed the effect of the composition on the conductivity of CZTS thin films prepared by chemical spray pyrolysis method. The results showed that best film is obtained when the Cu ratio is close to the stoichiometric composition [Cu/ (Zn + Sn)=1 and Zn/Sn=1] as in sample CZTS₃. Chen et al. reported that a Cu-poor condition leads to the formation of Cu vacancies, which generate shallow acceptors in CZTS, whereas a Zn-rich condition suppresses the Cu substitutions at Zn sites, which increases deep acceptors [24].

Table 4: Results of Hall effect measurements.

CZTS RH(cm^3/C)	p (cm^{-3})	μ ($\text{cm}^2/\text{v.s}$)	ρ ($\Omega \cdot \text{cm}$)	σ ($\Omega \cdot \text{cm}$) ⁻¹	
CZTS ₁	9.381	6.65×10^{17}	0.432	21.7152	0.0460
CZTS ₂	5.824	10.72×10^{17}	1.483	3.9272	0.1221
CZTS ₃	0.938	66.54×10^{17}	2.211	0.4242	2.3573
CZTS ₄	1.881	33.18×10^{17}	1.775	1.0597	0.9436
CZTS ₅	14.015	4.45×10^{17}	0.971	14.4336	0.0692

CONCLUSIONS

Thin films of Cu₂ZnSnS₄ were deposited by spray pyrolysis method on clean preheated glass substrates at 400°C with different Cu/ (Zn + Sn) ratios. The XRD results showed that all films are polycrystalline in nature with tetragonal structure and preferred orientation along (112) plane. The XRD measurement showed that the stoichiometry causes a reduction in the content of secondary phases. The Raman spectra showed a major peak of CZTS at (330-335 cm^{-1}) which proves the formation kesterite phase of CZTS. All films exhibit high transmittance indicating that the photon absorption occurs predominantly via band to band transitions. The prepared films have high absorption coefficient ($\alpha > 10^4 \text{cm}^{-1}$) and energy band gap are very close to the optimum value of the band gap required for the absorber material in thin film solar cell. The range of Urbach energy of the prepared films is (387- 827) meV. The conductivity of the films is estimated by Hall measurement and its maximum value is $2.3573 (\Omega \cdot \text{cm})^{-1}$ for the film CZTS₃ which can be considered to be suitable for solar cell applications.

REFERENCES

[1] EIA, U. (2013). International Energy Outlook 2013. US Energy Information Administration (EIA).
 [2] K. Ito, T. Nakazawa, Electrical and optical properties of stannite-type quaternary semiconductor thin films, Jpn. J. Appl. Phys. 27 (1988) 2094-2097.
 [3] Nakayama, N. & Ito, K. (1996). Sprayed films of

stannite Cu₂ZnSnS₄. Applied Surface Science, 92, 171-175. 171

[4] Tanaka, K., Moritake, N., & Uchiki, H. (2007). Preparation of Cu₂ZnSnS₄ thin films by sulfurizing sol-gel deposited precursors. Solar Energy Materials and Solar Cells, 91(13), 1199-1201.
 [5] H. Katagiri, K. Jimbo, W.S. Maw, K. Oishi, M. Yamazaki, H. Araki, A. Takeuchi, Development of CZTS-based thin film solar cells, Thin Solid Films 517 (2009) 2455-2460.
 [6] Seol, J. S., Lee, S. Y., Lee, J. C., Nam, H. D., & Kim, K. H. (2003). Electrical and optical properties of Cu₂ZnSnS₄ thin films prepared by rf magnetron sputtering process. Solar Energy Materials and Solar Cells, 75(1), 155-162.
 [7] Tanaka, T., Nagatomo, T., Kawasaki, D., Nishio, M., Guo, Q., Wakahara, A., ... & Ogawa, H. (2005). Preparation of Cu₂ZnSnS₄ thin films by hybrid sputtering. Journal of Physics and Chemistry of Solids, 66(11), 1978-1981. 174
 [8] Hall, S. R., Szymanski, J. T., & Stewart, J. M. (1978). Kesterite, (Cu₂ (Zn, Fe) SnS₄), and stannite, (Cu₂ (Fe, Zn) SnS₄), structurally similar but distinct minerals. The Canadian Mineralogist, 16(2), 131-137.
 [9] Schorr, S. (2007). Structural aspects of adamantine like multinary chalcogenides. Thin Solid Films, 515(15), 5985-5991.
 [10] Y. B. Kishore Kumar, G. Suresh Babu, P. UdayBhakar, V. Sundara Raja, Solar Energy Materials and Solar Cells 93 (2009) 230.
 [11] Y. B. Kishore Kumar, P. Uday Bhaskar, G. Suresh Babu, V. Sundara Raja, Phys. Stat. Sol. (a) 207 (2010) 149.
 [12] A. V. Simashkevich, D. A. Sherban, L. I. Bruk, A. Coval, V. Fedorov, E. Bobeico, Yu. Usaty, Proc. of the 20th European Solar Energy Conference, Vol. I (2005) 980.
 [13] Nabeel A. Bakr, Ziad T. Khodair and Shahlaa M. Abdul Hassan, Effect of Substrate Temperature on Structural and Optical Properties of Cu₂ZnSnS₄ (CZTS) Films Prepared by Chemical Spray Pyrolysis Method, Research Journal of Chemical Sciences, Vol. 5, Issue 10, pp. 51-61, October, (2014).
 [14] Nabeel A. Bakr, Ziad T. Khodair and Hussein I. Mahdi, Influence of Thiourea Concentration on some Physical properties of Chemically Sprayed Cu₂ZnSnS₄ Thin Films, International Journal of Materials Science and Application, Vol. 5, No. 6, pp. 261-270, (2016).
 [15] H. Park, Y.H. Hwang, B.-S. Bae, Sol gel processed Cu₂ZnSnS₄ thin films for photovoltaic absorber layer without sulfurization, J. Sol Gel. Sci. Technol. 65 (2013) 23-27.
 [16] B.D. Cullity, Elements of X-ray Diffraction, Addison-

Wesley, London, 1978, pp. 81–143.

- [17] VD Mote, Y Purushotham and BN Dole, Williamson-Hall analysis in estimation of lattice strain in nanometer-sized ZnO particles, *Journal of Theoretical and Applied Physics*, Vol. 6, pp. 1-8, (2012).
- [18] R. Touati, M. Ben Rabeh and M. Kanzari, Structural and optical properties of the new absorber Cu₂ZnSnS₄ thin films grown by vacuum evaporation method, *Energy Procedia*, Vol. 44, pp. 44-51, (2014).
- [19] M. Altosaar, J. Raudoja, K. Timmo, M. Danilson, M. Grossberg, J. Krustok, E. Mellikov, Cu₂Zn_{1-x}Cd_xSn(Se_{1-y}Sy)₄ solid solutions as absorber materials for solar cells, *Phys. Status. Solidi A* 205 (2008) 167-170.
- [20] P. A. Fernandes, P. M. P. Salome, A. F. da Cunha, *Journal of Alloys and Compounds* 509 (2011) 7600.
- [21] X. Fontané, V. Izquierdo-Roca, E. Saucedo, S. Schorr, V.O. Yukhymchuk, M.Ya. Valakh, A. Pérez-Rodríguez, J.R. Morante, *Journal of Alloys and Compounds* 539 (2012) 190.
- [22] M.J. _S_cepanski_c, M. Gruji_c-Broj_cin, Z.D. Doh_cevi_c-Mitrovi_c, Z.V. Popovi_c, Characterization of anatase TiO₂ nanopowder by variable-temperature raman spectroscopy, *Sci. Sinter.* 41 (2009) 67-73.
- [23] J. Tauc, R. Grigorovici, A. Vancu, Optical Properties, Electronic Structure, Of amorphous germanium, *Phys. Status. Solidi B* 15 (1966) 627-637.
- [24] S. Chen, X.G. Gong, A. Walsh, S. Wei, Defect physics of the kesterite thin-film solar cell absorber Cu₂ZnSnS₄, *Appl. Phys. Lett.* 96 (2010) 021902.